Research

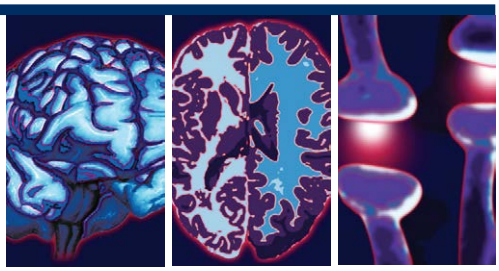

Demyelination takes Place Prior to Neuronal Damage following Intracerebroventricular Injection of Amyloid-Beta Oligomer (AβO)

Mao Zhang, Jie Zhang, Weiwei Zhang, Zhongxiang Yao†

ABSTRACT

Amyloid-beta (Aβ) peptide, commonly associated with Alzheimer's disease (AD), is known as a threat to neurons. However, the effect of Aβ peptide on myelin and oligodendrocytes (OLs) hasn't been exclusively discussed. In this study, a low concentration of amyloid-beta oligomer (AβO) was intracerebroventricularly injected to mice at the 2nd week. Body weight and motor coordination of mice were monitored during 8 weeks. Thioflavin-S (Th-S) staining, cresyl violet staining and immunostaining were supplied to assess Aβ deposits, neuronal damage, myelin disruption and activation of inflammatory glias following AβO injection. To identify the underlying cause of AβO-induced demyelination, AβO was administrated to oligodendrocyte precursor cells (OPCs) *in vitro*. In addition, OPCs can differentiate into myelinating cells----OLs. It showed that AβO not only suppressed the increase of body weight, but also resulted in the dysfunction of motor coordination in mice. Besides, neuronal damage was found in hippocampus, corpus callosum (CC) and cortex at the 8th week, but not at the 3rd week. Especially, neurofilament loss in the CC was developed until the 8th week, while demyelination was developed as early as the 3rd week. About other glias, AβO simply increased the amounts of astrocytes and microglias at the 8th week, but had no effect on them at the 3rd week. *In vitro*, AβO induced the decrease of oligodendrocyte amount and restriction of myelin basic protein $(MBP)^+$ membrane areas. This study proves that demyelination develops earlier than neuronal damage under AβO attack. Furthermore, it is supposed that the early detriment of AβO in myelin may further endanger neurons, and AβO-induced injury of OLs may facilitate this process. Relatively, the improvement of AβO-induced myelin damage at the early stage and the promotion of OLs may alleviate neuronal impairment, especially in AD.

Keywords:

Amyloid-beta oligomer (AβO), Demyelination, Neuronal damage, Oligodendrocytes (OLs), Neurons

Abbreviations

A2B5: Antigen of Oligodendrocyte-type-2 Astrocyte Progenitor Cell; AD: Alzheimer's Disease; Novas: Two-Way Analyses of Variance; Anti-A2B5: Anti-Antigen of Oligodendrocyte-Type-2 Astrocyte Progenitor Cell; Anti-GFAP: Anti-Glial Fibrillary Acidic Protein; Anti-AIF: Anti-Allograft Inflammatory Factor 1; Anti-MBP: Anti-Myelin Basic Protein; Anti-Neu N: Anti-Neuronal Nuclei; Anti-NF200: Anti-Neurofilament 200; Anti-NG2: Anti-Neuron-Glia Antigen 2; AP: Anteroposterior;

Department of Physiology, Army Medical University (Third Military Medical University), Chongqing 400038, China

†Author for correspondence: Zhongxiang Yao, Department of Physiology, Army Medical University (Third Military Medical University), Chongqing 400038, China, Tel: +86-23-68752247; email: yaozhx@yahoo.com

APP/PS1: $App_{swe}/PS1_{M146L}$; AIF-1: Allograft Inflammatory Factor 1; Aβ: Amyloid-Beta; Aβo: Amyloid-Beta Oligomer; BSA: Bovine Serum Albumin; CC: Corpus Callosum; CNS: Central Nervous System; DAB: 3,3-Diaminobenzadine; DAPI: 4,6-Diamidino-2-Phenylindole; DMEM/F12: Dulbecco's Modified Eagle Media / Nutrient Mixture F-12; DMSO: Dimethyl Sulfoxide; Dnase: Deoxyribonuclease; FBS: Fetal Bovine Serum; FITC: Fluorescein Isothiocyanate; GFAP: Glial Fibrillary Acidic Protein; HFIP: 1,1,1,3,3,3-Hexafluoroisopropanol; IP: Intraperitoneal; IPP: Image-Pro Plus; LTP: Long-Term Potentiation; MBP: Myelin Basic Protein; MCT: Monocarboxylate Transporter; MRI: Magnetic Resonance Imaging; Neu N: Neuronal Nuclei; NF200: Neurofilament 200; NG2: Glia Antigen 2; OD: Optical Density; OPC: Oligodendrocyte Precursor Cell; Opcs: Oligodendrocyte Precursor Cells; Ols: Oligodendrocytes; PBS: Phosphate-Buffered Saline; PDL: Poly-D-Lysine; PFA: Paraformaldehyde; $PS1_{M146V}$: Presenilin-1 $_{M146V}$; PVDF: Polyvinylidene Fluoride Membranes; ICC: Immuocytochemistry; SD: Standard Deviation; SDS-PAGE: Sodium Dodecyl Sulfate Polyacrylamide Gel Electrophoresis; TBS: Tris-Buffered Saline; TBST: Tris-Buffered Saline Containing 0.1% Tween 20; Th-S: Thioflavin-S; 3xtg-AD: The Triple Transgenic Mouse Model Of Alzheimer's Disease

Introduction

Myelin was first understood to enable 'saltatory' impulse propagation in axons more than 60 years ago, and this function is a key concept of neurophysiology [1]. Also, myelin is essential to establish connectivity in growing brain and higher-order cognitive functions, through which synchronized information can be transferred across neuronal system [2]. Besides, myelin integrity is crucial for the physiology of central nervous system (CNS), and required for long-term integrity and survival of axons [3]. Indeed, intact myelin can not only increase the resistance (and lower the capacitance) of axonal membranes, but also communicate with axons [4-6]. As an example, myelination can be enhanced in response to electrical excitation and activity-dependent molecular cascades. This reaction can protect the axons from damage, and significantly increase the speed of nerve impulse transmission [2,7].

In a study of Alzheimer's disease (AD), dystrophic neurites associated with amyloid-beta (Aβ) plaques was found to be demyelinated in cortical grey matter, and such plaque-associated demyelination was supposed to impair the function of cortex [8]. Actually, demylination was reported 20 years ago in a patient who suffered from memory and constructive apraxia [9]. Moreover, demyelination is boosted by Aβ peptide in AD-afflicted human brains [10-12]. Again, it was suggested that Aβ peptide may play a crucial role in the pathogenesis of white matter, according to the findings from T1-weighted magnetic resonance imaging (MRI) [13]. Also, in sporadic and preclinical AD cases, a focal demyelination and loss of oligodendrocytes (OLs) were found to be associated with Aβ plaque cores [14]. This association was further confirmed in an AD mouse model----$APP_{Swe}/PS1_{M146L}$ (APP/PS1) mice [15]. In the triple transgenic mouse model of AD (3xTg-AD), it not only harbors three AD-related genetic loci: human presenilin-1 $_{M146V}$ ($PS1_{M146V}$), human APP_{swe}, and human $tauP_{301L}$, but also develops Aβ plaques and neurofibrillary tangle-like pathology in a progressive and age-dependent manner [16]. Particularly, Aβ plaques, augmented by PS1 mutation, can induce oligodendrocyte dysfunction in 3xTg-AD mouse model [17]. Especially, significant alterations were observed in overall myelination patterns at time point preceding the appearance of amyloid and tau pathology in 3xTg-AD mouse model [18]. Otherwise, the inducer of overall change in myelin hasn't been identified. Besides, this appearance was simply identified in AD mouse model, but not observed in wild type mice. Therefore, it might be necessary to explore the direct reaction of myelin to Aβ attack in wild type mice *in vivo*.

Chronic demyelination can induce neuronal impairment, which subsequently leads to severe and permanent disability of the CNS [19]. Thus, fast restoration of myelin (remyelination) is crucial for circumventing demyelination-caused pathologies [20]. Implantation of exogenous remyelinating cells has been considered as a potential strategy for remyelination [21,22]. In addition, upon transplantation, isolated oligodendrocyte progenitors migrate throughout the injured white matter tracts, and then largely promote their remyelination [23]. Unfortunately, Aβ peptide can induce dysfunction and death of OLs both *in vivo* and *in vitro* [17,18,24]. Also, amyloid-beta oligomer (AβO) is toxic to neuronal cells and instigates neuronal damage in AD [25,26].

Especially, AβO may impair myelin integrity [8] which is essential for motor coordination [27].

Besides, the function of motor coordination is normally assessed by Rota-rod test [28,29]. Meanwhile, hippocampus and cortex are brain areas that mainly function in learning and memory [30]. Also, the impairment of corpus callosum (CC) was found to be associated with cognitive and learning dysfunction [31,32]. Therefore, to clearly reveal the underlying relation between Aβ-induced demyelination and neuronal damage, we chiefly assessed body weight, motor coordination via Rota-rod test, neuronal amounts in hippocampus and cortex, and neurofilament integrity in the CC following AβO injection. To identify a possible time lag existed between demyelination and neuronal damage, myelin basic protein (MBP) and neurofilament 200 (NF200) were double stained at the 3rd week and the 8th week respectively. Besides, the activation of astrocytes and microglias was additionally evaluated. At last, to explore the toxicity of AβO in OLs, oligodendrocyte precursor cells (OPCs) were administrated by AβO *in vitro*. Then, the amount of mature OLs and MBP^+ membrane expansion were further assessed.

Subjects and Methods

■ Subjects

To check the effect of AβO on neurons, myelin and inflammatory glias *in vivo*, AβO was administrated to 6-week-old C57BL/6 wild type mice by intracerebroventricular injection. *In vitro*, AβO was added to the cultured OPCs to identify its effect on cell amount and expansion of cell membrane. Besides, OPCs were purified from mixed cells using neonatal Sprague-Dawley rats. All animals were purchased from the Experimental Animal Center of the Third Military Medical University. Thirty C57BL/6 mice weighing 18.26 ± 0.31g were randomly divided into three groups (n=10/group). Similarly, cultured OPCs were grouped into three (n=5/group). The groups were named as control, sham and AβO groups.

All experiments in this study were performed in accordance with the Regulations for the Administration of Affairs Concerning Experimental Animals approved by the State Council of People's Republic of China. All animal experiments were approved by the Animal Ethical and Experimental Committee of the Army Medical University (Chongqing, Permit No. 201104) in accordance with their rules and regulations. All surgery was performed under pentobarbital sodium anesthesia, and all efforts were made to minimize suffering.

■ Reagents and Antibodies

Aβ1-42 (Sigma, St. Louis, MO, USA), 1,1,1,3,3,3-hexafluoroisopropanol (HFIP; Santa Cruz, California, USA) and dimethyl sulfoxide (DMSO; Sigma, St. Louis, MO, USA) was applied to prepare stoke solution of Aβ. Phosphate buffered saline (PBS, pH 8.5) was used to dilute stoke solution in order to produce AβO. Further, western blot was applied to evaluate the success of AβO generation. Sodium dodecyl sulfate polyacrylamide gel electrophoresis (SDS-PAGE; Beyotime, Nanjing, Jiangsu, China), polyvinylidene fluoride membranes (PVDF; Merck Millipore, Darmstadt, Germany), tris-buffered saline (TBS; Beyotime, Nanjing, Jiangsu, China), tris-buffered saline containing 0.1% tween 20 (TBST; Beyotime, Nanjing, Jiangsu, China), anti-amyloid oligomer antibody (Abcam, Cambridge, UK), horseradish peroxidase conjugated secondary anti-rabbit antibody (Zhongshan, Beijing, China) and chemiluminescence ECL kit (Invitrogen, Carlsbad, California, USA) were used in this experiment. *In vivo*, thioflavin-S (Th-S; Sigma, St. Louis, MO, USA) was applied to identify the deposit of AβO in brain. Moreover, cresyl violet (Santa Cruz, California, USA) was used to stain neurons in hippocampus. Neuronal amount in cortex and neurofilament integrity in the CC were further checked by immunostaining.

Dulbecco's modified eagle media/nutrient mixture F-12 (DMEM/F12; Hyclone, Logan, Utah, USA), fetal bovine serum (FBS; Hyclone, Logan, Utah, USA), N2-supplement (Invitrogen, Carlsbad, California, USA), deoxyribonuclease (DNase; Sigma, St. Louis, MO, USA), insulin (Sigma, St. Louis, MO, USA) and poly-D-lysine (PDL; Sigma, St. Louis, MO, USA) were used to purify OPCs. N-acetyl-L-cysteine (Amresco, Solon, OH, USA) and triiodothyronine (Sigma, St. Louis, MO, USA) were applied to oligodendrocyte precursor cell (OPC) differentiation.

1% albumin from bovine serum (BSA; Sigma, St. Louis, MO, USA) in 0.4% Triton X-100 (Sigma, St. Louis, MO, USA) was used as blocking buffer. Primary antibodies, including goat anti-myelin basic protein (anti-MBP; Santa Cruz, California, USA), rabbit anti-neurofilament 200 (anti-NF200; Sigma, St. Louis, MO, USA), rabbit anti-neuronal nuclei (anti-Neu N; Abcam, Cambridge, UK), mouse

anti-glial fibrillary acidic protein (anti-GFAP; Sigma, St. Louis, MO, USA), rabbit anti-allograft inflammatory factor 1 (anti-AIF-1; Invitrogen, Carlsbad, California, USA), rabbit anti-neuron-glia antigen 2 (anti-NG2; Merck Millipore, Darmstadt, Germany), and rabbit anti-antigen of oligodendrocyte-type-2 astrocyte progenitor cell (anti-A2B5; Merck Millipore, Darmstadt, Germany) were used for immunostaining. Anti-goat fluorescein isothiocyanate (FITC; Invitrogen, Carlsbad, California, USA) or anti-rabbit Cy3 labeled secondary antibodies (Merck Millipore, Darmstadt, Germany) were used for immunofluorescent staining. Nuclei were labeled by 4',6-diamidino-2-phenylindole (DAPI; Sigma, St. Louis, MO, USA). Alternatively, biotinylated anti-rabbit or anti-mouse secondary antibodies (Vector Laboratories, Burlingame, CA, USA) and 3,3-diaminobenzadine (DAB, Zhongshan, Beijing, China) were used for immunohistochemistry. Nuclei were labeled by haematoxylin (Zhongshan, Beijing, China).

■ AβO preparation and identification

In the AβO group, Aβ1-42 was used to generate AβO. In detail, Aβ1-42 was dissolved in HFIP to a final concentration of 1 mg/ml at 37 °C for 3 days, and then vacuum dried for 1 h. Until the generation of aliquoted peptides, DMSO was used to dissolve them to a final concentration of 1 mM. Subsequently, the stock was directly diluted into PBS (pH 8.5) to 50 μM and incubated at 4 °C for 24 h to generate AβO. The preparation of AβO is according to Chormy *et al* [33], and the success of AβO production was further assessed by western blot, characterized as Sebollela *et al* and Teng Wang *et al* [34,35]. In addition, PBS, used in the sham group, was subjected same manufacture as AβO preparation. To evaluate the success of AβO generation *in vitro*, we applied western blot to quantify AβO levels in the AβO group and the sham group, using an antibody targeting AβO peptides [36]. As results showed, AβO is successfully produced in the AβO group, and its molecular weight ranges from 30 to 100 KDa which is consistent with the study of Olivier Nicole *et al* [37]. Moreover, the OD value of immunoblot in the AβO group is comparatively higher than that of the sham group (83333 ± 11590 vs. 0 ± 0) (n=3, $^{**}p<0.01$) (Supplementary data 1).

■ Weighing and Rota-rod test

General condition of mice was assessed by monitoring their body weight and carrying out Rota-rod test during 8 weeks. More specifically, mice were weighed every day at 12:00. The daily weight was recorded to subtract the initial weight, and the deviation is defined as relative weight. Rota-rod test was applied to monitor motor coordination and balance of mice every other day during 8 weeks. In detail, 3 trials were applied at 13:00 for 3 consecutive days before Rota-rod test began. The mice were placed on a rotating cylinder (YLS-4C, Biowill co, Ltd, China), speed of which was accelerated from 5 to 40 revolutions per minute (rpm) and then kept at 40 rpm. The trial was considered finish once mouse fell off or gripped rungs and spun for two continuous circles [38]. All mice were evaluated on the Rota-rod three times a day. The time animals stayed on the cylinder was recorded and defined as maintain time. Besides, the longer of maintain time represents the better motor coordination and balance of mice [27,38].

■ AβO injection and Thioflavin-S staining

To get the model of AD [39], we supplied an intracerebroventricular injection of AβO as previously described by Balducci *et al* [40]. During the experiment, mice in the AβO group were injected with AβO (3 μl/3 min) at the concentration of 50 μM into the right lateral ventricle at stereotaxic coordinates: anteroposterior (AP) relative to bregma, −1.0 mm; lateral (L) to midline, 1.3 mm; ventral (V) from the skull surface, −2.0 mm [37]. The time point of injection is the 2nd week (the 14th day). Simultaneously, mice in the sham group were injected with the same amount of PBS (3 μl/3 min) using an identical manner. Additionally, mice in the control group weren't subjected any management **(Figure 1a)**.

To identify AβO deposits in the brain, Thioflavin-S (Th-S) was used to stain brain sections of mice at the 2nd day after injection. Th-S staining was carried out in sections mounted on gelatin-coated slices as previously described [41]. After dehydration in ethanol batteries, slices were incubated in distilled water for 10 min and then immersed in the Th-S solution (0.1% Th-S in 70% ethanol) for 8 min. Then, slices were washed twice in 70% ethanol for 30 seconds and cover-slipped. Th-S burden was observed by a fluorescence microscope (Olympus, Tokyo, Japan) **(Figure 1b)**.

■ Culture of oligodendrocyte precursor cells *in vitro* and AβO treatment

OPCs were propagated by the method from Jianqin Niu [42]. Briefly, the brains of P1～P3

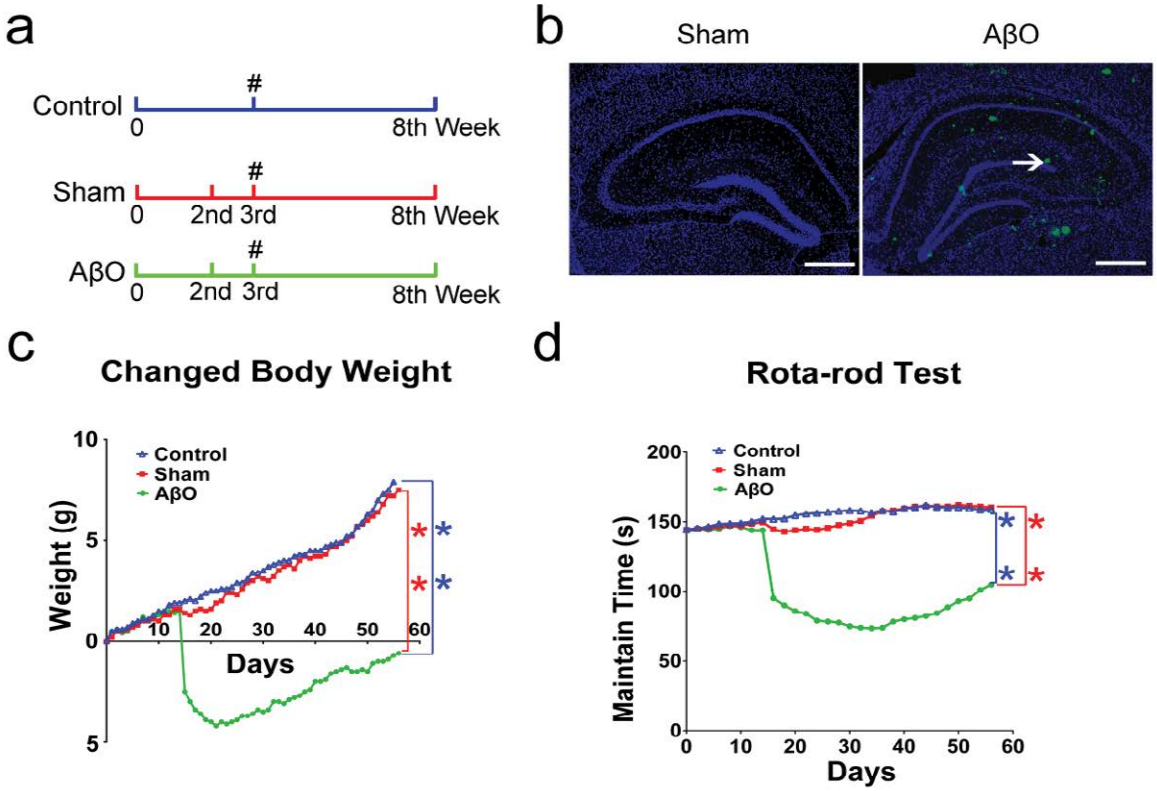

Figure 1: Body weight and motor coordination of mice are suppressed by amyloid-beta oligomer (AβO). (a) Mice from control, sham and AβO groups were administrated differently. The control group wasn't given any administration during whole of 8 weeks. Phosphate buffered saline (PBS) and AβO were intracerebroventricularly injected to mice in the sham group and the AβO group respectively at the 2nd week (the 14th day). The mark of "#" represents that 5 mice from each group were randomly chosen to identify the change of myelin and neurofilaments in corpus callosum (CC) at the 3rd week. Moreover, the results were analyzed at length in figure 3. At the 8th week, all of the mice were used for further observation in the aspect of myelin and neurofilaments, revealed in figure 4. (b) Thioflavin-S (Th-S) staining was supplied to confirm the success of AβO injection, and one of AβO deposits was pointed by arrowhead. (c) The change of relative weight was recorded during 8 weeks. At the 8th week, an increase of relative weight was found both in the control group and the sham group, and there are no significant differences between these two groups (n=5; $p>0.05$). Otherwise, AβO results in the decrease of relative weight at the 8th week in comparison with the control group (n=5; $^{**}p<0.01$) and the sham group (n=5; $^{**}p<0.01$). (d) To assess motor coordination of mice in each group, maintain time that mice kept their balance on a high-speed rod was recorded. There are no differences between the control group and the sham group (n=5; $p>0.05$). Besides, maintain time of the AβO group is significantly decreased at the 2nd week. Although a stable level is reached at the 8th week, it is still lower than those of the control group (n=5; $^{**}p<0.01$) and the sham group (n=5; $^{**}p<0.01$). Scale bar: B: 100μm.

Sprague-Dawley rats were used for mixed cell culture using mixed medium (DMEM/F12 + 10% FBS) for 5 days. Then, in order to get large quantity of OPCs, the mixed cells were cultured in OPC-proliferation medium (DMEM/F12 + 15% B104-conditioned medium + 1% N2-supplement) for another 5～7 days. Moreover, the cells were incubated with OPC-isolation medium (DMEM/F12 + 0.01% EDTA + 0.2 mg/mL DNase + 5 mg/mL insulin) for 15-30 min at 37°C and centrifuged (1000 r/min, 106g) for 5 min. To get purified OPCs, the pellets (morphology of OPCs) were suspended with the OPC-proliferation medium and seeded into T-25 flasks coated with PDL for propagation. The cells can be induced to differentiation by transferring medium into OPC-differentiation medium (DMEM/F12 + 1% N2-supplement +5 mg/mL N-acetyl-L-cysteine + 15 nmol/L triiodothyronine + 1% FBS +5 mg/mL insulin). All experiments were carried out using cells from the first passage. The ingredients of OPC mediums are listed in **Table 1**. To assess AβO-induced quantitative and morphological changes of OLs, 500 μL of single-cell suspension was plated into 24-well plates with coated glass cover slips and incubated in OPC-proliferation medium for 12h. Cells were then divided into three groups and given different administrations. The control group was incubated only with OPC-differentiation medium. According to Horiuchi *et al* [43], AβO at the final concentration of 10 μM was additionally added to OPCs in the AβO group. Relatively, equal volume of PBS was added to cells in the sham group. OPCs were cultured for another 4 days

Table 1: Medium ingredients.	
Medium	**Ingredients of Medium**
Mixed Medium	DMEM/F12 + 10% FBS
OPC-proliferation Medium	DMEM/F12 + 15% B104 Supernatant +1% N2
OPC-isolation Medium	DMEM/F12 + 0.01% EDTA + 0.2mg/mL DNase + 5μg/mL insulin
OPC-inoculation Medium	50% OPC-proliferation + 50% Mixed Medium
OPC-differentiation Medium	DMEM/F12 + 1% N2 + 5 mg/mL N-acetyl-L-cystine +15 nmol/L T3 +1% FBS + 5μg/mL insulin

with a complete change of medium and drugs every other day. At last, cells on glass cover slips were fixed with 4% paraformaldehyde (PFA) for immuocytochemistry (ICC).

■ Tissue processing and cresyl violet staining

Mice were anesthetized by intraperitoneal (IP) injection with 1% sodium pentobarbital. Then, mice were quickly transcardially perfused with 37 °C PBS followed by a slow perfusion with Zamboni's fixative for tissue fixation. Brain tissues were postfixed overnight at 4°C in Zamboni's fixative and then stored in 30% sucrose at 4°C for cryoprotection. Coronal sections (20μm) were obtained using a cryostat (Leica Camera AG, Solms, Germany) and collected in Zamboni's fixative.

Sections from bregma -2.18 to -2.3 mm (n=5/group) were used for 1% cresyl violet staining. After 3-min staining of cresyl violet, sections were differentiated in acetic acid ethanol for 5 seconds. Then, the sections were covered with resin (Sigma, St. Louis, MO, USA). The number of intact pyramidal cells per mm length of hippocampal CA1 and CA3 in both hemispheres was calculated. The results are expressed as the average number of cells within each frame per section.

■ Immunofluroscence, Immunohistochemistry, Morphometric Analysis and Quantification

Frozen brain samples were coronally sectioned from bregma +1.1 to +0.5 mm. Sections were incubated with 1% BSA in 0.4% Triton X-100 for 30 min at 37 °C, and then incubated overnight at 4 °C with goat anti-MBP (1:200) or rabbit anti-NF200 (1:200) antibodies, followed by FITC- or Cy3-conjugated secondary antibodies (1:500). Similarly, Cells were incubated with rabbit anti-NG2 (1:200), rabbit anti-A2B5 (1:100) or goat anti-MBP (1:200) antibodies respectively, followed by FITC- or Cy3-labeled secondary antibodies (1:500). For negative controls, incubation with primary antibodies was replaced by PBS. Nuclear counter stain was carried out using DAPI.

Free-floating sections from bregma +1.1 to +0.5 mm were incubated with primary antibodies, including rabbit anti-Neu N (1:100), mouse anti-GFAP (1:100) and rabbit anti-AIF-1 (1:200) antibodies, at 4 °C overnight. Following 15 min wash in PBS, sections were incubated with biotinylated anti-rabbit or anti-mouse secondary antibodies, and colored by DAB. Nuclei were carried out using haematoxylin.

The immunoreactivity was determined at 200× magnifications on a fluorescence microscope (Olympus, Tokyo, Japan) and a confocal laser-scanning microscope (Olympus, Tokyo, Japan). The total number of immunopositive cells per section was calculated in three non-contiguous sections (every 5th section) of the brain, and at least nine representative fields were randomly acquired at 200× magnification [44]. Morphometric analysis of OLs was performed using the Sholl analysis on the Pro Plus image analysis system by using standard concentric circles to evaluate the diameter and area of oligodendroglia [45]. Briefly, the program superimposes a grid of five concentric circles with increasing radii on an oligodendrocyte cell body, and then measures the number of intersections and the membrane expansion generated by OLs with each circle. At least nine representative fields were randomly acquired at 400× magnifications from each group performed in triplicate.

■ Statistical Analysis

The data are expressed as the mean ± standard deviation (SD). The body weight and maintain time that mice stayed on cylinder in Rota-rod test were analyzed using the Friedman Test. The data from immunofluroscence and immunohistochemistry were analyzed using one-way analysis of variance (ANOVA). The result of western blot was quantified by Image J software (NIH). Statistical analyses were performed using Prism 6 (GraphPad Prism Software Inc., La Jolla, CA, USA). The image-pro plus 6.0 (IPP 6.0) software was used to quantify photographs. Differences are considered statistical significance at a value of $^{*}p < 0.05$ and $^{**}p < 0.01$.

Results

■ Body weight and motor coordination of mice are suppressed by AβO

During 8 weeks, mice were tested for body weight and motor coordination. Relative weights of mice in the control group and the sham group are gradually increased from the beginning to the 8th week, which are increased by 7.9 ± 1.2 g and 7.5 ± 0.9 g at the 8th week respectively. Meanwhile, relative weight of the AβO group is gradually increased from the beginning and then obviously decreased at the 1st day after AβO injection. Next, it is gradually increased from the 3rd week to the 8th week following a transient drop. At the 8th week, relative weight of the AβO group is still decreased by 0.6 ± 0.3 g in comparison with the initial level (0.0 ± 0.0). There are no differences in relative weights between the control group and the sham group at the 8th week (n=5; $p>0.05$). However, relative weight of the AβO group is less than those of the control group (n=5; $^{**}p<0.01$) and the sham group (n=5; $^{**}p<0.01$) at the 8th week **(Figure 1c)**.

Rota-rod test is widely applied to check motor coordination of mice. The time that mice maintained their balance on the accelerating and high-speed cylinder was recorded. Mice in the control group and the sham group kept their balance well and seldom gripped the rungs. Moreover, the range of maintain time during 8 weeks varies from 144.53 ± 1.10 s to 160.73 ± 0.81 s in the control group, and varies from 144.23 ± 1.36 s to 162.17 ± 0.76 s in the sham group. In particular, averages of maintain times are 155.20 ± 0.83 s in the control group and 151.90 ± 0.03 s in the sham group during 8 weeks. Otherwise, maintain time of the AβO group is decreased from the initial level (143.33 ± 1.53 s) to 95.00 ± 1.00 s at the 1st day after AβO treatment, which is continuously decreased and then reaches 78.33 ± 0.58 s at the 5th week. Gradually, maintain time is slightly increased from the 5th week (78.33 ± 0.58 s) to the 8th week (101.16 ± 0.78 s). No differences were found between the control group and the sham group at the 8th week (n=5; $p>0.05$), maintain times of which are both longer than that of the AβO group (n=5; $^{**}p<0.01$) **(Figure 1d)**.

■ AβO-induced neuronal damage spreads in hippocampus, corpus callosum and cortex

To explore possible cognitive impairment resulted from AβO, hippocampus and cortex that take parts in learning and memory [27] were observed in the aspect of neuronal amount. Also, integrity of neurofilaments was further evaluated by immunofluorescent staining in the CC. Afterwards, AβO results in neuronal loss and neurofilament disruption at the 8th week, analyzed by cell counting and optical density (OD) value. Obviously, neuronal damage can be found in hippocampus, CC and cortex. Specifically, cresyl violet-stained sections in the control group and the sham group are evenly stained light blue, and there are regularly shaped cell bodies in hippocampal CA1 and CA3. The amounts of surviving neurons are 103.00 ± 6.56 /100μm^2 (the control group) vs. 101.33 ± 10.80 /100μm^2 (the sham group) in CA1 and 92.33 ± 4.93 /100μm^2 (the control group) vs. 87.33 ± 8.08 /100μm^2 (the sham group) in CA3 respectively **(Figure 2a)**. However, many neurons in CA1 and CA3 are damaged in the AβO group, showing irregularly aligned or shrunken somata and pyknotic nuclei. The surviving neurons in CA1 and CA3 are decreased to 76.00 ± 6.24 /100μm^2 and 65.00 ± 7.80 /100μm^2 in the AβO group. In comparison with the control group, there are no differences of neuronal amounts in the sham group (n=5; $p>0.05$), while a marked loss of neurons was found in the AβO group (n=5; $^{*}p<0.05$) **(Figure 2a)**.

NF200-positive neurofilaments in the CC are intact in the control group and the sham group, showing continuous neuronal fibers and similar OD values (9697.0 ± 620.0 vs. 10459.0 ± 1123.3) (n=5; $p>0.05$) **(Figure 2b)**. However, AβO leads to discontinuity and impairment of neurofilaments in the CC. Besides, there are differences in the OD values between the AβO group and the control group (5398.3 ± 379.0 vs. 9697.0 ± 620.0) (n=5; $^{*}p<0.05$) **(Figure 2b)**.

Neurons were labeled by Neu N and calculated by cell counting. Moreover, there are no differences between the control group and the sham group in neuronal amounts (104 ± 11 /100μm^2 vs. 99 ± 21 /100μm^2) (n=5; $p>0.05$). In contrast, there is a decrease of neuronal amount in the AβO group when compared with the control group (57 ± 12 /100μm^2 vs. 104 ± 11/100μm^2) (n=5; $^{*}p<0.05$) **(Figure 2b)**.

■ Demyelination takes place prior to neuronal damage and the activation of astrocytes and microglias

To explore the effect of AβO on myelin and its possible endangerment to neurofilaments, MBP and NF200 were double stained in the CC. As

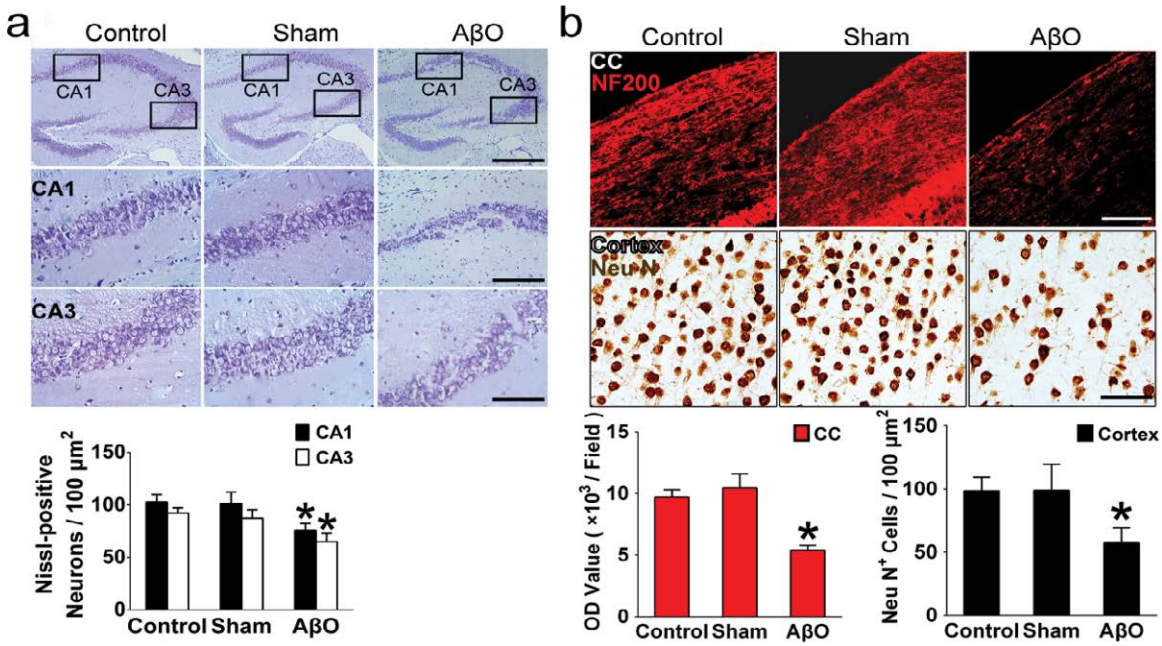

Figure 2: Neurons in hippocampus, corpus callosum (CC) and cortex are damaged by amyloid-beta oligomer (AβO) at the 8th week. (a) Hippocampal neurons were stained by cresyl violet. Similar amounts of neurons were found in the control group and the sham group at the 8th week (n=5; $p>0.05$). Otherwise, there is a decrease of neuronal amount in the AβO group when compared with the control group at the 8th week (n=5; $*p<0.05$). (b) Neuronal axons in the CC and neurons in cortex were labeled by neurofilament 200 (NF200) and neuronal nuclei (Neu N) respectively. Intact and continuous neurofilaments in the CC were found both in the control group and the sham group, showing no differences in optical density (OD) values (n=5; $p>0.05$). Conversely, AβO results in the disruption of neurofilaments, and there are obvious differences in OD values between the control group and the AβO group (n=5; $*p<0.05$). Neurons, labeled by Neu N, are regularly arranged in the control group and the sham group, and no differences in neuronal amounts were found between these two groups (n=5; $p>0.05$). All the same, there is an obvious loss of neuronal amount in the AβO group in comparison with the control group (n=5; $*p<0.05$). Scale bars: A: 100μm, 50μm; B: 50μm, 25μm.

results showed, myelin and neurofilaments are intact in the control group and the sham group both at the 3rd week and the 8th week. However, unparallel changes of myelin and neurofilaments are found in the AβO group. Demyelination takes place both at the 3rd week and the 8th week, while neurofilament loss is developed just at the 8th week **(Figures 3 and 4)**.

Specifically, there are no differences in the OD values of MBP and NF200 at the 3rd week between the control group and the sham group (n=5; $p>0.05$): the OD values of MBP and NF200 are 13299.2 ± 2014.5 and 11165.2 ± 2592.9 in the control group; the OD values of MBP and NF200 are 11962.3 ± 1561.3 and 10817.6 ± 3116.9 in the sham group. Notably, AβO results in the downregulation of MBP at the 3rd week in comparison with that of the control group (9116.8 ± 1204.8 vs. 13299.2 ± 2014.5) (n=5; $*p<0.05$) **(Figure 3)**. Otherwise, neurofilaments are not obviously disrupted by AβO at the 3rd week, showing the similar expression of NF200 as the control group (10265.3 ± 987.9 vs.11165.2 ± 2592.9) (n=5; $p>0.05$) **(Figure 3)**.

At the 8th week, similar OD values of MBP and NF200 were found in the control group and the sham group (n=5; $p>0.05$): the OD values of MBP and NF200 are 13411.0 ± 692.0 and 9697.0 ± 613.6 in the control group; the OD values of MBP and MF200 are 11642.3 ± 572.4 and 10459.3 ± 1123.3 in the sham group. In addition, there still exist differences in MBP expressions between the AβO group and the control group at the 8th week (7716.3 ± 653.7 vs. 13411.0 ± 692.0) (n=5; $*p<0.05$) **(Figure 4)**. Importantly, the expression of NF200 is downregulated in the AβO group when compared with that of the control group at the 8th week (5398.3 ± 397.0 vs. 9697 ± 613.6) (n=5; $*p<0.05$) **(Figure 4)**.

Demyelinating neurons are fragile to the menace from inflammation. To identify whether inflammation was stimulated after AβO treatment, activated astrocytes and microglias were statistically evaluated both at the 3rd week and the 8th week **(Figure 5)**. Glial fibrillary acidic protein (GFAP) and allograft inflammatory factor 1 (AIF-1) were used to label astrocytes and microglias respectively.

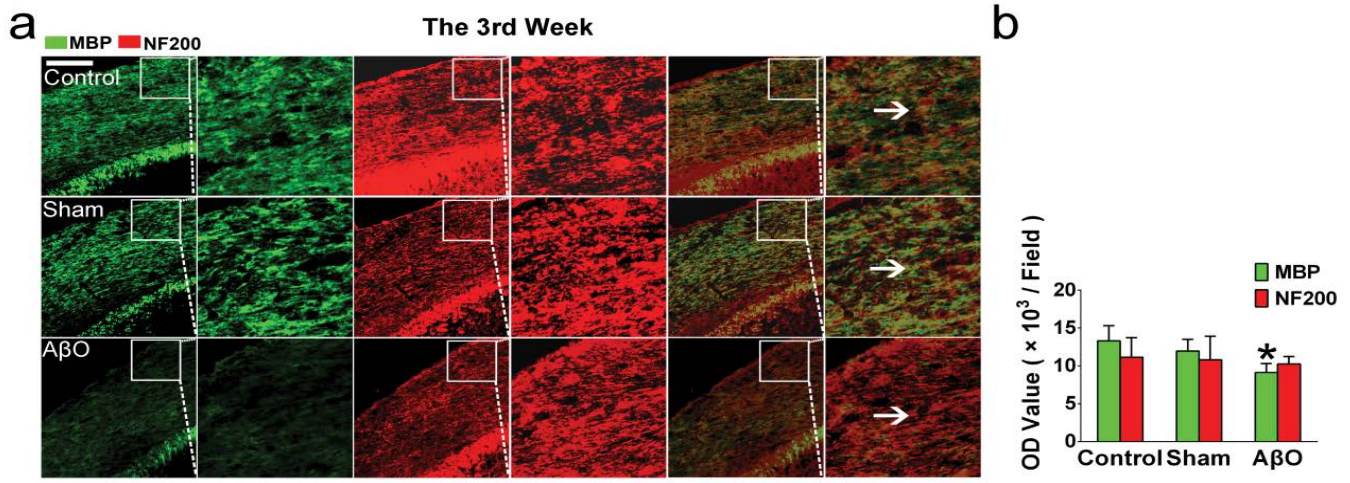

Figure 3: Amyloid-beta oligomer (AβO)-induced demyelination occurs at the 3rd week in corpus callosum (CC). (a) Through double staining of myelin basic protein (MBP, green) and neurofilament 200 (NF200, red), it showed that AβO leads to demyelination, but does not induce obviously neurofilament loss at the 3rd week, as arrowheads pointed. (b) At the 3rd week, there are no differences in MBP and NF200 expressions between the control group and the sham group (n=5; *p>0.05)*. However, AβO leads to the downregulation of MBP expression in comparison with the control group (n=5; **p<0.05*). Besides, there are no differences in NF200 expression between the AβO group and the control group (n=5; *p>0.05)*. Scale bars: A: 50μm; B: 50μm.

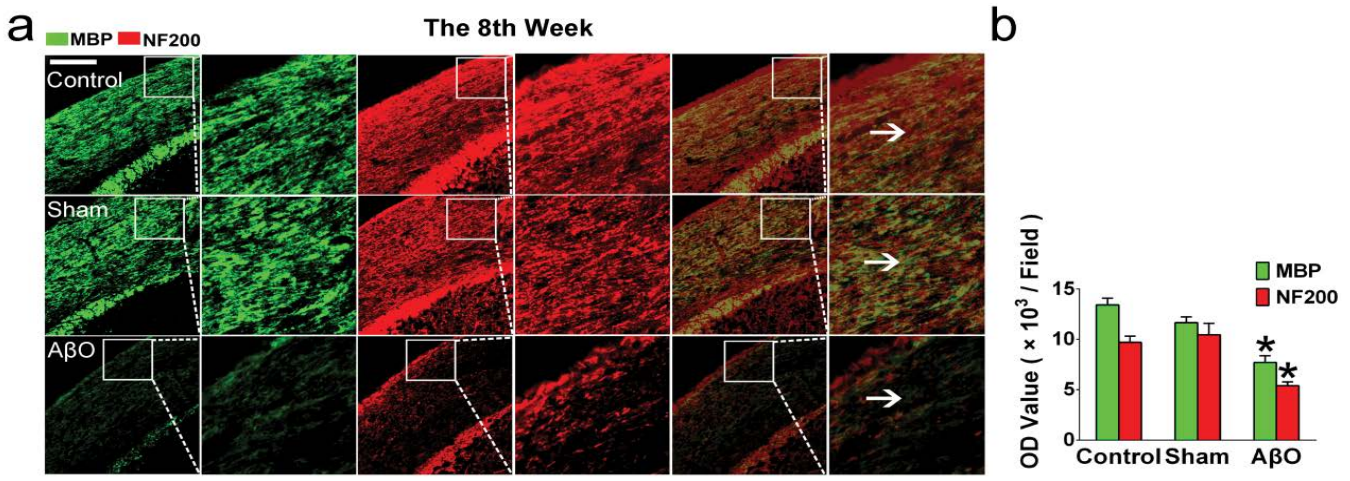

Figure 4: Amyloid-beta oligomer (AβO) disrupts integrities of myelin and neurofilaments at the 8th week in corpus callosum (CC). (a) Myelin basic protein (MBP, green) and neurofilament 200 (NF200, red) were double labeled to check myelin and neurofilaments in the CC at the 8th week. As arrowheads pointed, AβO not only induces myelin disruption, but also leads to neurofilament loss. (b) Statistically, no differences were found between the control group and the sham group in expressions of MBP and NF200 (n=5; *p>0.05)*. Otherwise, both of MBP and NF200 expressions are downregulated in the AβO group when compared with the control group (n=5; **p<0.05*). Scale bars: A: 50μm; B: 50μm.

At the 3rd week, there are no differences of GFAP and AIF-1 expressions among the control group, the sham group and the AβO group (n=5; **p>0.05*) **(Figure 5a)**. Statistically, the quantities of GFAP+ and AIF-1+ cells are 32.00 ± 6.24 /100μm² and 10.00 ± 2.00 /100μm² in the control group, which have no differences with those of the sham group (31.33 ± 11.01 /100μm² and 12.67 ± 3.21 /100μm²) (n=5; *p>0.05*) **(Figure 5b)**. Also, no differences were found between the control group and the AβO group in the amounts of GFAP+ and AIF-1+ cells, which are 32.00 ± 6.24 /100μm² and 10.00 ± 2.00 /100μm² in the control group vs. 30.00 ± 9.17 /100μm² and 12.00 ± 2.65 /100μm² in the AβO group (n=5; *p>0.05*) **(Figure 5b)**.

At the 8th week, in comparison with the control group, there is an obvious increase of GFAP and AIF-1 expressions in the AβO group (n=5; **p<0.05*), and a subtle change of GFAP and AIF-1 expressions in the sham group (n=5; *p>0.05*) **(Figure 5c)**. In statistic, the numbers of GFAP+ and AIF-1+ cells in the AβO group are 57.00 ± 13.53 /100μm² and 25.67 ± 6.66

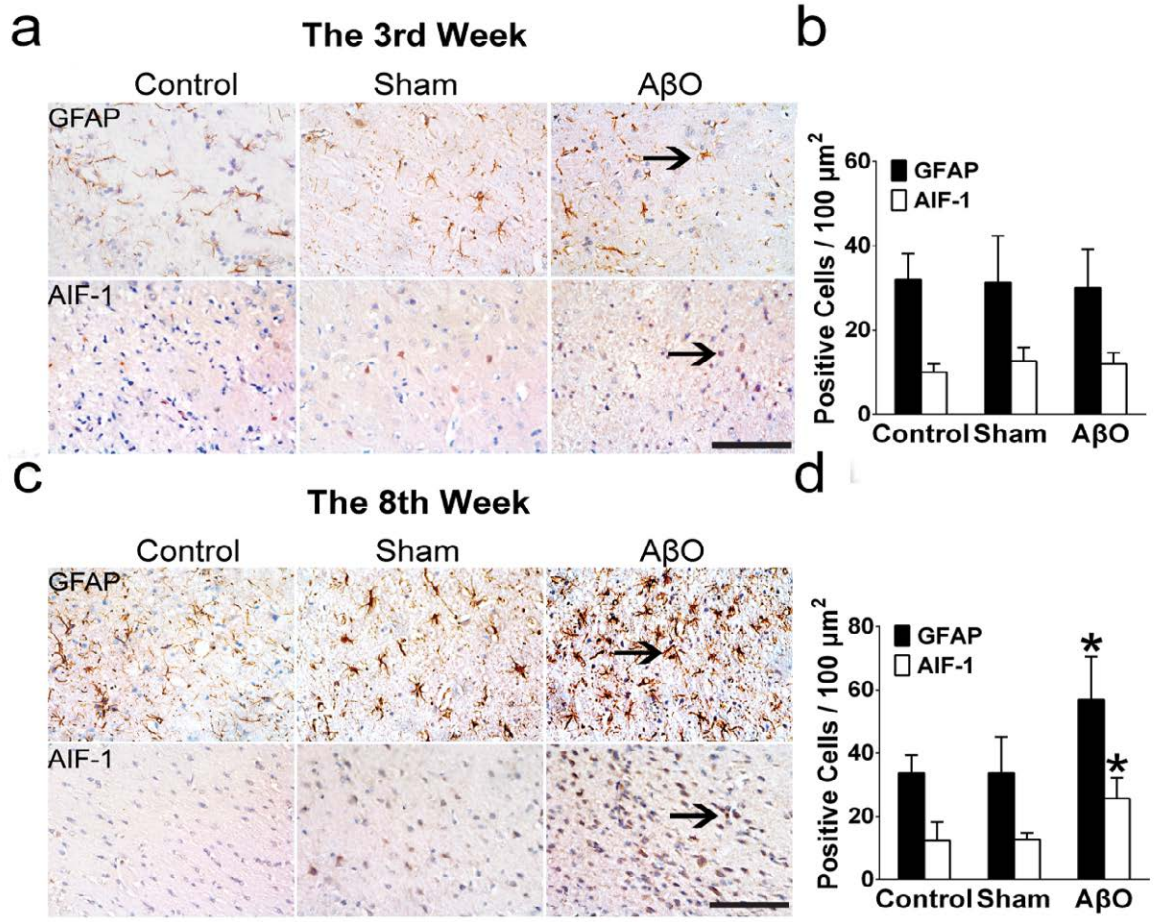

Figure 5: Amounts of astrocytes and microglias are increased at the 8th week, but not at the 3rd week. Glial fibrillary acidic protein (GFAP) and allograft inflammatory factor 1 (AIF-1) were used to label astrocytes and microgilas respectively. (a) At the 3rd week, there are no changes of GFAP and AIF-1 expressions among control, sham and AβO groups. (b) Statistically, the amounts of GFAP+ and AIF-1+ cells have no differences in control, sham and AβO groups. (c) At the 8th week, there is an obvious increase of GFAP and AIF-1 expressions in the AβO group when compared with the control group. (d) In statistic, the quantities of GFAP+ and AIF-1+ cells in the AβO group are more than those of the control group (n=5; *$p<0.05$). Likewise, there are no differences in the amounts of GFAP+ and AIF-1+ cells between the control group and the sham group (n=5; $p>0.05$). Scale bar: A: 25μm.

/100μm², which are more than those of the control group (33.67 ± 5.69 /100μm² and 12.33 ± 5.86 /100μm²) (n=5; *$p<0.05$) (Figure 5d). Besides, the quantities of GFAP+ cells and AIF-1+ cells are 34.25 ± 11.50 /100μm² and 12.67 ± 2.08 /100μm² in the sham group vs. 33.67 ± 5.69 /100μm² and 12.33 ± 5.86 /100μm² in the control group. It shows no differences between these two groups (n=5; $p>0.05$) (Figure 5d).

■ The Amount of oligodendrocytes and MBP+ membrane areas are retarded by AβO *in vitro*

OPCs were purified from mixed cells *in vitro*, undergoing the stages of proliferation, prematuration and maturation, and then subjected to immunofluorescent staining (Figure 6a). What's more, the OPCs, labeled by neuron-glia antigen 2 (NG2), display small and ellipse cell bodies. Typically premature OLs which have symmetrical bipolar or tri-polar processes were labeled by antigen of oligodendrocyte-type-2 astrocyte progenitor cell (A2B5). OLs were labeled by MBP, showing netlike processes (Figure 6a). At mature stage, the amount and morphology of OLs were checked in control, sham and AβO groups via labeling MBP (Figure 6b). The amount of OLs in the AβO group is 28 ± 9 /100μm², which is less than that of the control group (39 ± 11 /100μm²) (n=5; *$p<0.05$). Otherwise, no significant differences exist between the control group (39 ± 11 /100μm²) and the sham group (41 ± 13 /100μm²) (n=5; $p>0.05$) (Figure 6c). Morphometric and quantitative analysis, performed on the expansion of MBP+ membrane area, clearly demonstrates that MBP+ membrane areas and sheet formation were weakened by AβO. Specifically, the normalized area of the AβO group is 13667 ±

4690 μm², which is less than that of the control group (19000 ± 5377 μm²) (n=5; *$p<0.05$). Alternatively, no differences were found between the control group (19000 ± 5377 μm²) and the sham group (21000 ± 5141 μm²) (n=5; $p>0.05$) **(Figure 6b, d)**.

Discussion

Aggregation of Aβ into oligomers, fibrils, and plaques plays a role in molecular pathogenesis of AD [46,47]. Again, AβO contributes to the disruption of synapses and neurotransmission, progressive neuronal death, memory impairment and cognitive disturbances [48-50]. In a novel model, Aβ acts as a trigger of cellular events, which not only leads to dementia with tau, but also mediates AD-related synaptic deficits [51,52]. Apparently, AβO may play an indispensable role in the progression of AD, while pre-existing studies mainly focus on its detriment to neurons. For instance, Aβ accumulation was proved to suppress synaptic transmission and plasticity *in vivo* [53-55], and refrain the survival of hippocampal neurons *in vitro* [56-58]. Similarily, in our study, it proves that intracerebroventricular injection of AβO not only suppresses the body weight and motor coordination of mice, but also induces neuronal damage in hippocampus, CC and

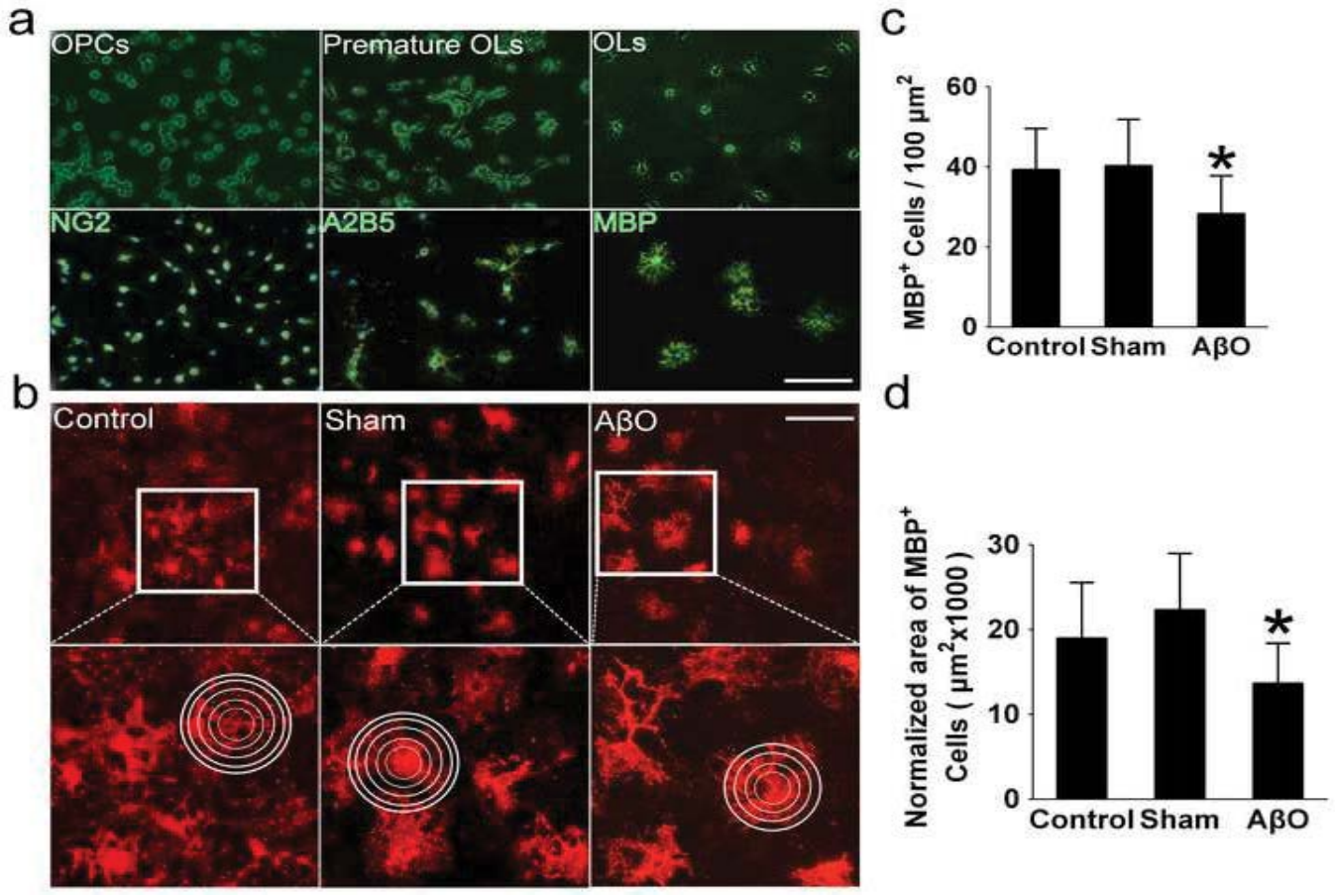

Figure 6: Amyloid-beta oligomer (AβO) inhibits the amount and membrane expansion of oligodendrocytes (OLs) *in vitro*. (a) Cultured oligodendrocyte precursor cells (OPCs) were purified from mixed cells *in vitro*. Generally, OPCs get through the stage of premature OLs, and then gradually differentiate into mature OLs. The morphologies of oligodendroglia lineage cells cultured *in vitro* at each stage were captured and shown in the figure. Again, immunofluorescent staining of oligodendrocyte markers at each stage was applied to identify the cell purity. As neuron-glia antigen 2 (NG2) labeled, the morphology of OPCs is compact and round. Premature OLs, labeled by antigen of oligodendrocyte-type-2 astrocyte progenitor cell (A2B5), display bipolar or tri-polar processes. Furthermore, mature OLs, labeled by myelin basic protein (MBP), are surrounded by amounts of processes. (b) To assess the effect of AβO on OLs (differentiated from OPCs) *in vitro*, OLs were labeled by MBP in control, sham and AβO groups. What's more, the amount of OLs and MBP⁺ membrane areas were calculated in these three groups. (c) Based on statistical analysis, the amount of MBP⁺ cells is decreased in the AβO group when compared with the control group (n=5; *$p<0.05$). Moreover, similar amounts of MBP⁺ cells are found in the control group and the sham group (n=5; $p>0.05$). (d) Membrane sheet area of MBP⁺ cells was quantified, and a reduction of MBP expansion membrane was found in the AβO group in comparison with the control group (n=5; *$p<0.05$). Meanwhile, there are no differences in MBP⁺ membrane areas between the control group and the sham group (n=5; $p>0.05$). Scale bar: 25μm.

cortex *in vivo*. Accordingly, AβO can lead to neuronal impairment, and then induce neuronal dysfunction in AD. More than this, Aβ plaques were found to be related with early demyelination and oligodendrocyte impairment [16,17,39]. However, the direct effect of Aβ on myelin hasn't been extensively explored, and requires further study. Especially, this effect might facilitate neuronal damage under Aβ attack.

Furthermore, we found that behavioral performance of mice becomes abnormal at the 1st day after AβO injection, while demyelination takes place after 1 week following AβO injection. This interesting phenomenon rightly testifies that behavioral abnormality is an acute and transient reaction of animals to AβO [59,60], while the impairment of AβO in myelin is a complicated process that requires a little more time [14]. Besides, deficits of behavioral performance may be a stress reaction to extraneous AβO injection, which can be affected by various factors such as changes of surroundings and body weight [61]. About AβO-induced demyelination, it is usually a consequence of a direct insult targeted at OLs [62], and its main pathologies are genetic abnormalities (leukodystrophies) and inflammatory damages [63,64]. Thus, detectable demyelination may require more time, and differ from rapid changes of signaling pathways. As an example, PI3K/Akt/GSK3 and MAPK/ERK1/2 pathways can be rapidly activated and detected early following AβO injection [65,66]. Moreover, related compensatory mechanisms may exist in the process of demyelination, one of which is repair function of OLs in myelin disruption. It was reported that OLs can generate new myelin in a few hours *in vivo* [67]. Therefore, obvious demyelination may occur later than behavioral abnormality after AβO treatment.

Injured myelin in vulnerable late-myelinating regions can release oligodendrocyte- and myelin-associated irons to promote Aβ oligomerization and exacerbate neuronal impairment [68]. Moreover, demyelination was recognized as a contributor of cognitive impairment in AD [12,69,70]. As neuroimaging showed, there is a greater loss of intact myelin developed in AD patients in comparison with controls [71]. Moreover, the loss of intact myelin precedes the onset of cognitive impairment [72]. Especially, myelin loss and degraded myelin vesicles, found in the white matter of AD brains, may be a threat to neuronal circuitry and cognitive function [73]. Also, it showed that Aβ administration depresses hippocampal long-term potentiation (LTP) [74]. Particularly, MBP, a specific marker of myelin, was previously nominated as a novel Aβ chaperone protein, which can potently inhibit Aβ fibril assembly *in vitro* [75]. Furthermore, the absence of MBP, e.g. demyelination, can promote neuroinflammation and glial activation, and this effect may speed up neuronal damage [76,77]. Based on these observations, it seems that myelin injury can facilitate the endangerment of Aβ to neurons, but still lacking sufficient evidences. Meanwhile, in our study, it reveals that AβO-induced demyelination takes place prior to axonal degeneration, and the disrupted myelin may further interact with the activation of inflammatory cells (astrocytes and microglias) *in vivo*. As a result, neuronal axons become more vulnerable to AβO *in vivo*. Therefore, it suggested that neural dysfunction may be directly resulted from neuronal toxicity of Aβ, and also indirectly facilitated by Aβ-induced myelin loss.

Furthermore, myelin loss can be repaired by OPCs which can rapidly and efficiently promote axonal remyelination [23]. In particular, OPCs can not only aid in restoring strong electrochemical communication between synapses, but also in preventing axonal degeneration [29,78,79]. Besides, early pathology of OLs (differentiated from OPCs) in AD mice may be a novel therapeutic target [80]. Actually, in preclinical and presymptomatic AD, the loss and dysfunction of oligodendrocyte lineage cells are deemed the cause of long-lasting demyelination [81-83]. *In vitro*, Aβ not only leads to mitochondrial dysfunction and DNA fragmentation of OLs [84,85], but also disturbs myelin formation of OLs [86]. Hence, to reveal the underlying cause of Aβ-induced demyelination, we supplied AβO administration to the cultured OPCs *in vitro*. As a result, AβO reduces the amount of OLs (differentiated from OPCs), and also restricts membrane expansion of OLs. So, it suggested that early demyelination and impairment of OLs may facilitate and accelerate neuronal impairment under AβO attack.

Actually, OLs can also metabolically support axons in energy supplement other than forming myelin around axons [87]. In particular, a metabolic cycle may exist in OLs, astrocytes and neurons [88], and OLs are quite sensitive to energy depletion [89,90]. Besides, the metabolic support of neurons can be facilitated by lactate shuttle from OLs to axons [91,92]. As an energy metabolite, lactate is transported

by monocarboxylate transporter (MCT) family, and three members of them (MCT1, MCT2 and MCT4) are expressed in the brain [93,94]. MCT1 is specifically expressed in OLs and its expression is highly associated with neuronal growth [44,95]. Thus, it suggested that AβO may impede lactate shuttle between OLs and neurons via disturbing MCT1 expression. Again, AβO can lead to the incapability of OLs in remyelination. As a result, neuronal axons become more vulnerable to AβO injury. More than this, AβO has a directly toxic effect on OPCs, which can suppress the proliferation of OPCs, decrease the quantity of OLs and further restrict membrane expansion of OLs. As a result, the intact of myelin is disrupted, which leads to the exposure of neuronal axons to AβO, aggravating neuronal damage under AβO attack **(Figure 7)**.

Here, this study primarily reveals that AβO results in the decrease of body weight and dysfunction of motor coordination *in vivo*. Then, it further identifies that AβO induces neuronal damage in brain areas including hippocampus, CC and cortex. Most importantly, this study recognizes that AβO can induce myelin impairment at an early stage, and early demyelination may be a contributor to axonal degeneration. In addition, as previous studies found [76,77], inflammatory cells (astrocytes and microglias) are activated as well. In particular, AβO-induced demyelination may be mainly contributed by the toxic effect of AβO on myelinating cells----OLs. As our results showed, AβO actually reduces oligodendrocyte amount and restricts membrane expansion of OLs (differentiated from OPCs) *in vitro*. Thus, it suggested that myelin loss can accelerate neuronal

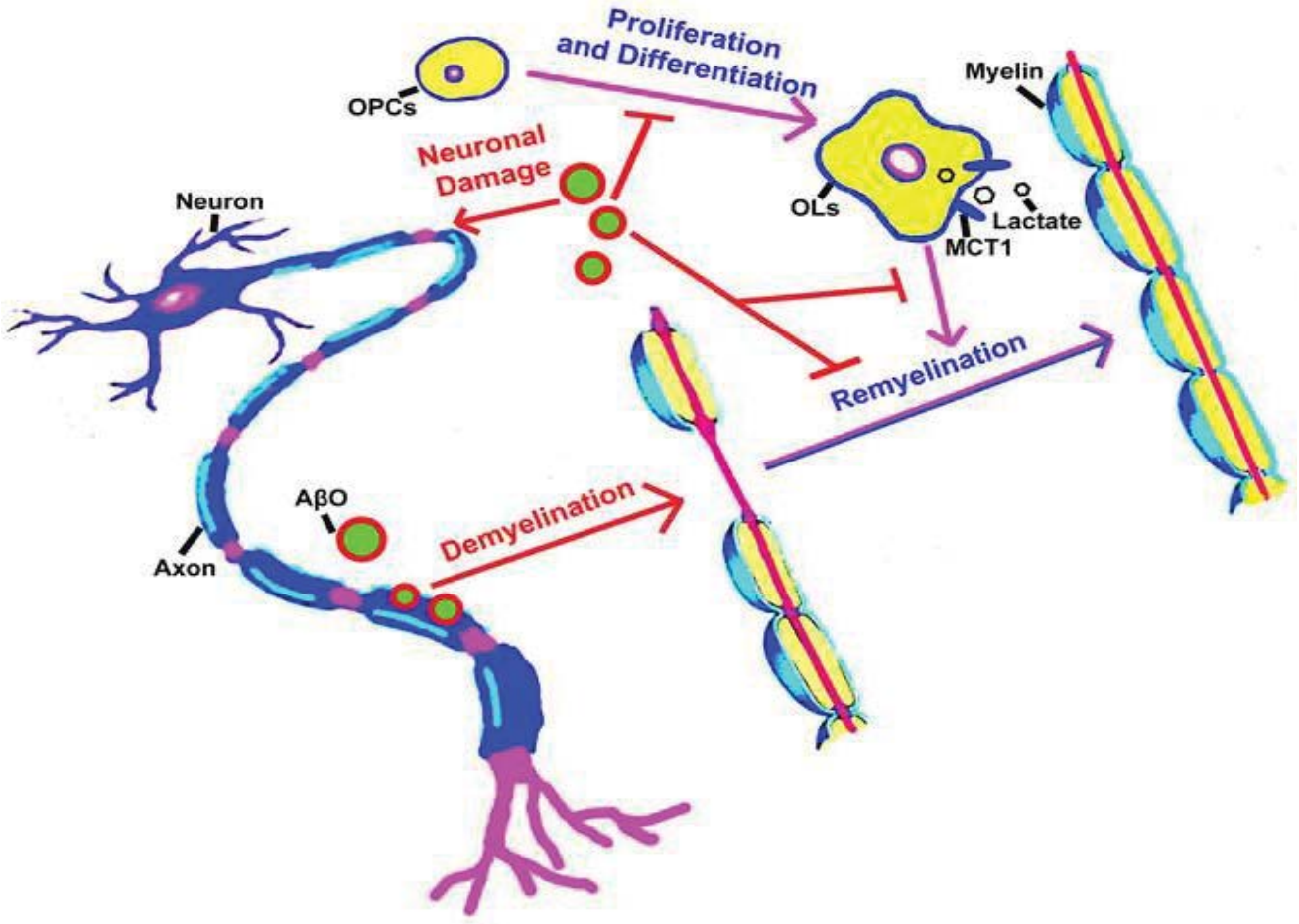

Figure 7: Early demyelination may exacerbate neuronal damage under AβO attack. This effect may be related with the suppression of AβO in OLs. Demyelination takes place prior to neuronal damage following AβO administration, and this early demeylination makes neurons largely expose to AβO. Consequently, neurons become more vulnerable to AβO attack. Furthermore, AβO-induced damage of OLs may contribute to the long-lasting demyelination. More specifically, AβO may inhibit the proliferation of OPCs, decrease the amount of OLs, and also restrict membrane expansion of OLs. Through these effects, OLs become incapable to facilitate remyelinaiton. In combination with previous studies [95,96], the underlying mechanism of AβO-induced neuronal damage may also associate with MCT1 expression in OLs. More specifically, AβO may suppress MCT1 expression of OLs, which can disturb lactate shuttle between OLs and neurons, leading to energy deficiency of neurons. "↓" represents "from one stage to the next stage", "⊥" stands for "suppression".

damage when facing AβO endangerment. What's more, this process may be facilitated by the AβO-induced impairment of OLs. Furthermore, the changing trend in the amounts of neural cells, observed in this study, is parallel to that of AD post-mortem human brains: the amounts of OLs and neurons are decreased and astrocyte amount is increased [96].

Based on these evidences, this study mainly explains the possible association between the early demyelination and neuronal damage, and provides a new insight that timely restoration of myelin and promotion of OLs may benefit AβO-induced neuronal damage, especially in AD. Otherwise, in current work, we just observed the phenomenon of AβO-induced early demylination and later neuronal injury, and AβO-induced impairment of OLs *in vitro*. But, this study hasn't directly and deeply checked the direct and protective role of promoting remyelination and oligodendrocyte survival in neuronal damage. Also, we have mentioned that amelioration of lactate supplement in neurons can alleviate neuronal injury in aspect of energy supplement. Actually, myelin surrounding neuronal axons and OLs can provide lactate to neurons, further alleviating neuronal lactate deficit and promoting neuronal survival [44,95]. Otherwise, this work hasn't further recognized the change of lactate metabolism in AD, and possible links between OLs and neurons. Thus, it is still waiting for further exploration in the positive effects of OLs and myelin on neurons in aspects of direct neuronal protection from AβO attack, energy metabolism and other underlying regulating role [97].

Acknowledgements

This work was supported by grants from the National Natural Science Foundation of China (Grant No. 31371147).

References

1. Geren BB, Raskind J. Development of the fine structure of the myelin sheath in sciatic nerves of chick embryos. *Proc. Natl. Acad. Sci. USA* 39(1), 880-884 (1953).
2. Yakovler PI, Lecours AR. The myelogenetic cycles of regional maturation of the brain. In: Minkowski A. eds. Regional development of the brain in early life. F. A. Davis Co. Philadelphia, 3-70 (1967).
3. Wang Y, Sun P, Wang Q, *et al.* Differentiation and quantification of inflammation, demyelination and axon injury or loss in multiple sclerosis. *Brain* 138(1), 1223-1238 (2015).
4. Griffiths I, Klugmann M, Anderson T, *et al.* Axonal swellings and degeneration in mice lacking the major proteolipid of myelin. *Science* 280(1), 1610-1613 (1998).
5. Edgar JM, McLaughlin M, Yool D, *et al.* Oligodendroglial modulation of fast axonal transport in a mouse model of hereditary spastic paraplegia. *J. Cell. Biol* 166(1), 121-131 (2004).
6. Yin X, Crawford TO, Griffin JW, *et al.* Myelin-associated glycoprotein is a myelin signal that modulates the caliber of myelinated axons. *J. Neurosci* 18(1), 1953-1962 (1998).
7. Wake H, Lee PR, Fields RD. Control of local protein synthesis and initial events in myelination by action potentials. *Science* 333(1), 1647-1651 (2011).
8. Stricker NH, Schweinsburg BC, Delano Wood L, *et al.* Decreased white matter integrity in late-myelinating fiber pathways in Alzheimer's disease supports retrogenesis. *Neuroimage* 45(1), 10-16 (2009).
9. Zahner B, Lang CJ, Engelhardt A, *et al.* A case of Alzheimer's disease with extensive focal white matter changes. *Dementia* 6(1), 294-300 (1995).
10. Firbank MJ, Blamire AM, Krishnan MS, *et al.* Atrophy is associated with posterior cingulate white matter disruption in dementia with Lewy bodies and Alzheimer's disease. *Neuroimage* 36(1), 1-7 (2007).
11. Roher AE, Weiss N, Kokjohn TA, *et al.* Increased A beta peptides and reduced cholesterol and myelin proteins characterize white matter degeneration in Alzheimer's disease. *Biochemistry* 41(1), 11080-11090 (2002).
12. Bartzokis G. Age-related myelin breakdown: a developmental model of cognitive decline and Alzheimer's disease. *Neurobiol. Aging* 25(1), 5-18 (2004).
13. Sachdev PS, Zhuang L, Braidy N, *et al.* Is Alzheimer's a disease of the white matter? *Curr Opin. Psychiatry* 26(1), 244-251 (2013).
14. Mitew S, Kirkcaldie MT, Halliday GM, *et al.* Focal demyelination in Alzheimer's disease and transgenic mouse models. *Acta. Neuropathol* 119(1), 567-577 (2010).
15. Borchelt DR, Ratovitski T, van Lare J, *et al.* Accelerated amyloid deposition in the brains of transgenic mice coexpressing mutant presenilin 1 and amyloid precursor proteins. *Neuron* 19(1), 939-945 (1997).
16. Mastrangelo MA, Bowers WJ. Detailed immunohistochemical characterization of temporal and spatial progression of Alzheimer's disease-related pathologies in male triple-transgenic mice. *BMC. Neurosci* 9(1), 81 (2008).
17. Desai MK, Guercio BJ, Narrow WC, *et al.* An Alzheimer's disease-relevant presenilin-1 mutation augments amyloid-beta-induced oligodendrocyte dysfunction. *Glia* 59(1), 627-640 (2011).
18. Desai MK, Mastrangelo MA, Ryan DA, *et al.* Early oligodendrocyte/myelin pathology in Alzheimer's disease mice constitutes a novel therapeutic target. *Am. J. Pathol* 177(1), 1422-1435 (2010).
19. Czepiel M, Boddeke E, Copray S. Human oligodendrocytes in remyelination research. *Glia* 63(1), 513-530 (2015).
20. Franklin RJ, Ffrench Constant C. Remyelination in the CNS: From biology to therapy. *Nat. Rev. Neurosci* 9(1), 839-855 (2008).
21. Martino G, Franklin RJM, Baron Van Evercooren A, *et al.* Stem cell transplantation in multiple sclerosis: Current status and future prospects. *Nat. Rev. Neurol* 6, 247-255 (2010).
22. Goldman SA, Nedergaard M, Windrem MS. Glial progenitor cell-based treatment and modeling of neurological disease. *Science* 338(1), 491-495 (2012).
23. Wegener A, Deboux C, Bachelin C, *et al.* Gain of Olig2 function in oligodendrocyte progenitors promotes remyelination. *Brain* 138(1), 120-135 (2015).

24. Lee JT, Xu J, Lee JM, *et al.* Amyloid-beta peptide induces oligodendrocyte death by activating the neutral sphingomyelinase-ceramide pathway. *J. Cel.l Biol* 164(1), 123-131 (2004).

25. Kirsten L. Viola, William L. Klein. Amyloid β oligomers in Alzheimer's disease pathogenesis, treatment, and diagnosis. *Acta. Neuropathologica* 129(1), 183-206 (2015).

26. Park J, Choi H, Min JS, *et al.* Loss of mitofusin 2 links beta-amyloid-mediated mitochondrial fragmentation and Cdk5-induced oxidative stress in neuron cells. *J. Neurochem* 132(1), 687-702 (2015).

27. Liebetanz D, Merkler D. Effects of commissural de- and remyelination on motor skill behaviour in the cuprizone mouse model of multiple sclerosis. *Exp. Neurol* 202(1), 217-224 (2006).

28. Ye JN, Chen XS, Su L, *et al.* Progesterone alleviates neural behavioral deficits and demyelination with reduced degeneration of oligodendroglial cells in cuprizone-induced mice. *PLoS. One* 8(1), e54590 (2013).

29. Zhang M, Zhan XL, Ma ZY, *et al.* Thyroid hormone alleviates demyelination induced by cuprizone through its role in remyelination during the remission period. *Exp. Biol. Med* 240(1), 1183-1196 (2015).

30. Cha HJ, Kim YJ, Jeon SY, *et al.* Neurotoxicity induced by alkyl nitrites: Impairment in learning/memory and motor coordination. *Neurosci. Lett* 619, 79-85 (2016).

31. Cui Z, Xia Z, Su M, *et al.* Disrupted white matter connectivity underlying developmental dyslexia: A machine learning approach. *Hum. Brain. Mapp* 37(1), 1443-1458 (2016).

32. Huang X, Du X, Song H, *et al.* Cognitive impairments associated with corpus callosum infarction: a ten cases study. *Int. J. Clin. Exp. Med* 8(1), 21991-219918 (2015).

33. Chromy BA, Nowak RJ, Lambert MP, *et al.* Self-assembly of Abeta(1-42) into globular neurotoxins. *Biochemistry* 42(1), 12749-112760 (2003).

34. Sebollela A, Mustata GM, Luo K, *et al.* Elucidating molecular mass and shape of a neurotoxic Aβ oligomer. *ACS. Chem. Neurosci* 5(1), 1238-1245 (2014).

35. Wang T, Xie XX, Ji M, *et al.* Naturally occurring autoantibodies against Ab oligomers exhibited more beneficial effects in the treatment of mouse model of Alzheimer's disease than intravenous immunoglobulin. *Neuropharmacology* 105(1), 561-576 (2016).

36. Faucher P, Mons N, Micheau J, *et al.* Hippocampal injections of oligomeric amyloid β-peptide (1-42) induce selective working memory deficits and long-lasting alterations of ERK signaling pathway. *Front. Aging. Neurosci* 7(1), 245 (2016).

37. Nicole O, Hadzibegovic S, Gajda J, *et al.* Soluble amyloid beta oligomers block the learning-induced increase in hippocampal sharp wave-ripple rate and impair spatial memory formation. *Sci. Rep* 2016(6), 22728 (2016).

38. Kuhlmann T, Miron V, Cui Q, Wegner C, Antel J, Bruck W. *et al.* Differentiation block of oligodendroglial progenitor cells as a cause for remyelination failure in chronic multiple sclerosis. *Brain* 131(1), 749-758 (2008).

39. Chambon C, Wegener N, Gravius A, *et al.* Behavioural and cellular effects of exogenous amyloid-beta peptides in rodents. *Behav. Brain. Res* 225(1), 623-641 (2011).

40. Balducci C, Beeg M, Stravalaci M, *et al.* Synthetic amyloid-beta oligomers impair long-term memory independently of cellular prion protein. *Proc. Natl. Acad. Sci. USA* 107(1), 2295-2300 (2010).

41. Espargaró A, Sabate R, Ventura S. Thioflavin-S staining coupled to flow cytometry. A screening tool to detect in vivo protein aggregation. *Mol. Biosyst* 8(1), 2839-2844 (2012).

42. Niu J, Mei F, Li N, *et al.* Haloperidol promotes proliferation but inhibits differentiation in rat oligodendrocyte progenitor cell cultures. *Biochem. Cell. Biol* 88(1), 611-620 (2010).

43. Horiuchi M, Maezawa I, Itoh A, *et al.* Amyloid β1-42 oligomer inhibits myelin sheet formation in vitro. *Neurobiol. Aging* 33(1), 499-509 (2012).

44. Zhang M, Ma ZY, Qin HC, *et al.* Monocarboxylate Transporter 1 in the Medial Prefrontal Cortex Developmentally Expresses in Oligodendrocytes and Associates with Neuronal Amounts. *Mol. Neurobiol* 54(3), 2315-2326 (2017).

45. Rajasekharan S, Baker KA, Horn KE, *et al.* Netrin 1 and Dcc regulate oligodendrocyte process branching and membrane extension via Fyn and RhoA. *Development* 136(1), 415-426 (2009).

46. Riverol M, López OL. Biomarkers in Alzheimer's disease. Front Neurol 2(1), 46 (2011).

47. Catafau AM, Bullich S. Amyloid PET imaging: applications beyond Alzheimer's disease. *Clin. Transl. Imaging* 3(1), 39-55 (2015).

48. González Marrero I, Giménez Llort L, Johanson CE, *et al.* Choroid plexus dysfunction impairs beta-amyloid clearance in a triple transgenic mouse model of Alzheimer's disease. *Front. Cell. Neurosci* 9(1), 17 (2015).

49. Tabuchi M, Lone SR, Liu S, *et al.* Sleep interacts with Aβ to modulate intrinsic neuronal excitability. *Curr. Biol* 25(1), 702-712 (2015).

50. Londos E, Passant U, Brun A, *et al.* Clinical Lewy body dementia and the impact of vascular components. *Int. J. Geriatr. Psychiatry* 15(1), 40-49 (2000).

51. Wang ZX, Tan L, Liu J, *et al.* The essential role of soluble Aβ oligomers in Alzheimer's disease. *Mol. Neurobiol* 53(1), 1905-1924 (2016).

52. Liao D, Miller EC, Teravskis PJ. Tau acts as a mediator for Alzheimer's disease-related synaptic deficits. *Eur. J. Neurosci* 39(1), 1202-1213 (2014).

53. Scala F, Fusco S, Ripoli C, *et al.* Intraneuronal Aβ accumulation induces hippocampal neuron hyperexcitability through A-type K(+) current inhibition mediated by activation of caspases and GSK-3. *Neurobiol. Aging* 36(1), 886-900 (2005).

54. Lian H, Yang L, Cole A, *et al.* Rodriguez Rivera J, Taglialatela G, Jankowsky JL, Lu HC, Zheng H. NFκB-activated astroglial release of complement C3 compromises neuronal morphology and function associated with Alzheimer's disease. *Neuron* 85(1), 101-115 (2015).

55. Ripoli C, Cocco S, Li Puma DD, *et al.* Intracellular accumulation of amyloid-β (Aβ) protein plays a major role in Aβ-induced alterations of glutamatergic synaptic transmission and plasticity. *J. Neurosci* 34(1), 12893-12903 (2014).

56. Lambert MP, Barlow AK, Chromy BA, *et al.* Diffusible, nonfibrillar ligands derived from Abeta1-42 are potent central nervous system neurotoxins. *Proc. Natl. Acad. Sci. USA* 95(1), 6448-6453 (1998).

57. Takei N, Sobu Y, Kimura A, *et al.* Cytoplasmic fragment of Alcadein α generated by regulated intramembrane proteolysis enhances amyloid β-protein precursor (APP) transport into the late secretory pathway and facilitates APP cleavage. *J. Biol. Chem* 290(1), 987-995 (2015).

58. Xing S, Shen D, Chen C, *et al.* Regulation of neuronal toxicity of β-amyloid oligomers by surface ATP synthase. *Mol. Med. Rep* 8(1), 1689-1694 (2013).

59. Prut L, Belzung C. The open field as a paradigm to measure the effects of drugs on anxiety-like behaviors: A review. *Eur. J. Pharmacol* 463(1), 3-33 (2003).

60. Ryan S Wong, David F Cechetto, Shawn N Whitehead. Assessing the effects of acute amyloid β oligomer exposure in the rat. *Int. J. Mol. Sci* 17(1), 1390 (2016).

61. Tamano H, Ide K, Adlard PA, *et al.* Involvement of hippocampal excitability in amyloid β-induced behavioral and psychological symptoms of dementia. *J. Toxicol. Sci* 41(1), 449-457 (2016).

62. Zawadzka M, Franklin RJ. Myelin regeneration in demyelinating disorders: new developments in biology and clinical pathology. *Curr. Opin. Neurol* 20(1), 294-298 (2007).

63. Mason JL, Langaman C, Morell P, *et al.*

Episodic demyelination and subsequent remyelination within the murine central nervous system: changes in axonal calibre. *Neuropathol. Appl. Neurobiol* 27(1), 50-58 (2001).

64. Franklin RJ, Ffrench Constant C. Remyelination in the CNS: from biology to therapy. *Nat. Rev. Neurosci* 9(1), 839-855 (2008).

65. Jimenez S, Torres M, Vizuete M, *et al.* Age-dependent accumulation of soluble amyloid beta (Abeta) oligomers reverses the neuroprotective effect of soluble amyloid precursor protein-alpha (sAPP(alpha)) by modulating phosphatidylinositol 3-kinase (PI3K)/Akt-GSK-3beta pathway in Alzheimer mouse. *J. Biol. Chem* 286(1), 18414-18425 (2011).

66. Morroni F, Sita G, Tarozzi A, *et al.* Early effects of Aβ1-42 oligomers injection in mice: Involvement of PI3K/Akt/GSK3 and MAPK/ERK1/2 pathways. *Behav. Brain. Res* 314(1), 106-115 (2016).

67. Czopka T, Ffrench Constant C, Lyons DA. Individual oligodendrocytes have only a few Hours in which to generate new myelin sheaths in vivo. *Dev. Cell* 25, 599-609 (2013).

68. Bartzokis G, Lu PH, Mintz J. Human brain myelination and amyloid beta deposition in Alzheimer's disease. *Alzheimers. Dement* 3(1), 122-125 (2007).

69. Wallin A, Gottfries CG, Karlsson I, *et al.* Decreased myelin lipids in Alzheimer's disease and vascular dementia. *Acta. Neurol. Scand* 80(1), 319-323 (1989).

70. Han X, MHD, McKeel DW Jr, *et al.* Substantial sulfatide deficiency and ceramide elevation in very early Alzheimer's disease: potential role in disease pathogenesis. *J. Neurochem* 82(1), 809-818 (2002).

71. Lee DY, Fletcher E, Martinez O, *et al.* Regional pattern of white matter microstructural changes in normal aging, MCI, and AD. *Neurology* 73(1), 1722-1728 (2009).

72. Bartzokis G, Cummings JL, Sultzer D, *et al.* White matter structural integrity in healthy aging adults and patients with Alzheimer disease: a magnetic resonance imaging study. *Arch. Neurol* 60(1), 393-398 (2003).

73. Zhan X, Jickling GC, Ander BP, *et al.* Myelin injury and degraded myelin vesicles in Alzheimer's disease. *Curr. Alzheimer. Res* 11(1), 232-238 (2014).

74. Kimura R, MacTavish D, Yang J, *et al.* Pramlintide antagonizes beta amyloid (Aβ)- and human amylin-induced depression of hippocampal long-term potentiation. *Mol. Neurobiol* 54 (1), 748 (2016).

75. Hoos MD, Ahmed M, Smith SO, *et al.* Inhibition of familial cerebral amyloid angiopathy mutant amyloid β-protein fibril assembly by myelin basic protein. *J. Biol. Chem* 282(1), 9952-9961 (2007).

76. Ou Yang MH, Van Nostrand WE. The absence of myelin basic protein promotes neuroinflammation and reduces amyloid β-protein accumulation in Tg-5xFAD mice. *J. Neuroinflammation* 10(1), 134 (2013).

77. Cunningham C, Hennessy E. Co-morbidity and systemic inflammation as drivers of cognitive decline: new experimental models adopting a broader paradigm in dementia research. *Alzheimers. Res. Ther* 7(1), 33 (2015).

78. McLean NA, Popescu BF, Gordon T, *et al.* Delayed nerve stimulation promotes axon-protective neurofilament phosphorylation, accelerates immune cell clearance and enhances remyelination in vivo in focally demyelinated nerves. *PLoS. One* 9(1), e110174 (2014).

79. Crawford AH, Chambers C, Franklin RJ. Remyelination: the true regeneration of the central nervous system. *J. Comp. Pathol* 149(1), 242-254 (2013).

80. Nielsen HM, Ek D, Avdic U, *et al.* NG2 cells, a new trail for Alzheimer's disease mechanisms? *Acta. Neuropathol. Commun* 1(1), 7 (2013).

81. Gold BT, Powell DK, Andersen AH, *et al.* Alterations in multiple measures of white matter integrity in normal women at high risk for Alzheimer's disease. *Neuroimage* 52(1), 1487-1494 (2010).

82. Ringman JM, O'Neill J, Geschwind D, *et al.* Diffusion tensor imaging in preclinical and presymptomatic carriers of familial Alzheimer's disease mutations. *Brain* 130(1), 1767-1776 (2007).

83. Zhang Y, Zou J, Yang J, *et al.* 4Aβ1-15-derived Monoclonal antibody reduces more Aβ burdens and neuroinflammation than homologous vaccine in APP/PS1 mice. *Curr. Alzheimer. Res* 12(1), 384-397 (2015).

84. Xu J, Chen S, Ahmed SH, *et al.* Amyloid-beta peptides are cytotoxic to oligodendrocytes. *J. Neurosci* 21(1), RC118 (2011).

85. Tarczyluk MA, Nagel DA, Rhein Parri H, *et al.* Amyloid β 1-42 induces hypometabolism in human stem cell-derived neuron and astrocyte networks. *J. Cereb. Blood. Flow. Metab* 35(1), 1348-1357 (2015).

86. Niu J, Mei F, Wang L, *et al.* Phosphorylated olig1 localizes to the cytosol of oligodendrocytes and promotes membrane expansion and maturation. *Glia* 60(1), 1427-1436 (2012).

87. Sanchez-Abarca LI, Tabernero A, Medina J M. Oligodendrocytes use lactate as a source of energy and as a precursor of lipids. Glia 36(1), 321-329 (2001).

88. Amaral AI, Meisingset TW, Kotter MR, *et al.* Metabolic aspects of neuron-oligodendrocyte-astrocyte interactions. *Front. Endocrinol* 4(1), 54 (2013).

89. Foncin JF, Le Beau J. Myelinopathy due to carbon monoxyde poisoning. A study in ultrastructural neuropathology. *Acta. Neuropathol* 1978(43) 153-159 (1978).

90. Egan PJ, Becker FW, Schumm F. Spongiform leucoencephalopathy after inhaling illicit heroin and due to carbon monoxide-intoxication. *Fortschr. Neurol. Psychiatr* 72(1), 26-35 (2004).

91. Rinholm JE, Hamilton NB, Kessaris N, *et al.* Regulation of oligodendrocyte development and myelination by glucose and lactate. *J. Neurosci* 31(1), 538-548 (2011).

92. Rinholm JE, Bergersen LH. Neuroscience: The wrap that feeds neurons. *Nature* 487(1), 435-436 (2012).

93. Halestrap AP. The SLC16 gene family-structure, role and regulation in health and disease. *Mol. Aspects. Med* 34(1), 337-349 (2013).

94. Dienel GA, Hertz L. Glucose and lactate metabolism during brain activation. *J. Neuroscience. Res* 66(1), 824-838 (2001).

95. Lee Y, Morrison BM, Li Y, *et al.* Oligodendroglia metabolically support axons and contribute to neurodegeneration. *Nature* 487(1), 443-448 (2012).

96. Lasn H, Winblad B, Bogdanovic N. Neuroglia in the inferior olivary nucleus during normal aging and Alzheimer's disease. *J. Cell. Mol. Med* 10(1), 145-156 (2006).

97. Caballero E, Calvo Rodríguez M, Gonzalo Ruiz A, *et al.* A new procedure for amyloid β oligomers preparation enables the unambiguous testing of their effects on cytosolic and mitochondrial Ca^{2+} entry and cell death in primary neurons. *Neurosci. Lett* 612(1), 66-73 (2016).